Interaction of the Cationic Peptide Bactenecin with Phospholipid Monolayers at the Air-Water Interface: I Interaction with 1,2-Dipalmitoyl-sn-Glycero-3-Phosphatidilcholine

ARTICLE *in* THE JOURNAL OF PHYSICAL CHEMISTRY B · AUGUST 2009

Impact Factor: 3.3 · DOI: 10.1021/jp902709t · Source: PubMed

Interaction of the Cationic Peptide Bactenecin with Phospholipid Monolayers at the Air−Water Interface: I Interaction with 1,2-Dipalmitoyl-*sn*-Glycero-3-Phosphatidilcholine

A. B. López-Oyama,[†] A. L. Flores-Vázquez,[‡] M. G. Burboa,[†,§] L. E. Gutiérrez-Millán,[†,§] J. Ruiz-García,[‡] and M. A. Valdez*[,†,||]

Departamento de Investigación en Polímeros y Materiales, Departamento de Investigaciones Científicas y Tecnológicas, and Departamento de Física, Universidad de Sonora, Rosales y Transversal, 83000 Hermosillo, Sonora, México and Instituto de Física, Universidad Autónoma de San Luis Potosí, Alvaro Obregón 64, 78000 San Luis Potosí, SLP, México

Received: March 25, 2009; Revised Manuscript Received: May 23, 2009

In this work we have investigated the influence of NaCl on the adsorption of the antimicrobial cationic peptide bactenecin in the monolayer of 1,2-dipalmitoyl-*sn*-glycero-3-phosphocholine (DPPC) at the air−water interface, as a function of NaCl concentrations in the subphase. We show that the effect of the salt concentration on DPPC monolayers is a monotonic decrease of the liquid-condensed−liquid-expanded (LC-LE) coexistence region. By contrast, the effect of the bactenecin adsorption at the DPPC monolayer not only removed the LC-LE coexistence region plateau, but also shifted the DPPC isotherms to higher pressures and increased the compressibility of the DPPC/bactenecin monolayers with respect to the pure DPPC monolayer around the LC phase. Analysis of the domain structure, obtained by Brewster angle and atomic force microscopes, indicates that the salt concentration in the subphase builds an electrostatic barrier, increasing the rigidity of DPPC monolayers and limiting the bactenecin adsorption at the LC-LE phase coexistence.

1. Introduction

Antimicrobial peptides (AMPs) have been found in several different types of organisms: plants, insects, birds, crustaceans, amphibians, bacteria,[1−4] and even humans.[5,6] AMPs are important components of innate immunity, and their distribution throughout the animal kingdom is widespread, producing polypeptides that exert a direct toxic effect in vitro on bacteria and parasites, thereby presumably contributing to the defense mechanisms of the host against invading microorganisms.[7,8] AMPs play an important role in the host defense against bacteria and fungi; in particular, neutrophiles, eosinophiles, and macrophages, which constitute the major animal cell-dependent defense system, synthesize highly cationic polypeptides, which can cause a marked decrease in viability of a variety of organisms.[9,10] For some of these polypeptides, a mode of action has been reported that consists of an increase in the permeability of the bacterial membrane or an inhibition of bacterial DNA synthesis.[4,7] AMPs are a unique and diverse group of molecules on the basis of their amino acids composition and structure; they exhibit potent activities against a rather broad spectrum of microbial organisms, including Gram-positive and Gram-negative bacteria, fungi, and enveloped viruses.[7] Hancock et al.[11] have proposed that cationic peptides first interact with bacteria by binding to their negatively charged surfaces, and for Gram-negative bacteria they act as outer membrane permeabilizers. Their interactions with the cytoplasmic membrane have been proposed to lead to the disruption of membrane structure, resulting in dissipation of the transmembrane potential and eventual cell death. On the basis of their secondary structure, cationic peptides can be categorized into four major groups, which include β-sheet structures stabilized by two to three disulfide bridges (defensins), α-helices (melittins), extended structures with a predominance of one or more amino acid (indolicidin), and loop-structure peptides containing only one disulfide bridge (bactenecin).[12,13] One of the most important group of these AMPs are the ones extracted from bovine neutrophiles, since in bovine neutrophiles the antibacterial activity is associated with a population of large granules, which are the predominant organelles in the cytoplasm of this cell type. This group of antimicrobial peptides includes bactenecin, which is the smallest natural cationic antimicrobial peptide of 12 amino acids; 4 arginine, 2 cysteine, and 6 other hydrophobic residues. The two cystein residues form a disulfide bond to make bactenecin a loop molecule. Bactenecins are peptides processed from precursors cathelicidins in large granules within polymorphonuclear neutrophiles.[11,14,15] It has been found that bactenecin has activity against Gram-positive, Gram-negative, and fungi. Furthermore, it has been demonstrated that bactenecin binds electrostatically to negatively charged lipopolysacharide molecules of the outer membrane of bacteria and then enter the cytoplasm and inhibit multiple intracellular targets.[11,12,14,16,17]

Biological membranes are one of the major constituents of living organisms and play an important role in structural organization and functioning of both prokaryotic and eukaryotic cells. The amphipathic nature of cell membanes permits them to assembly in very well structured forms. A long time ago, different models were proposed to mimic processes carried out by biological membranes, which have helped us to understand individual properties of particular components of the membrane. The peptide−membrane interaction can be analyzed through the interactions with vesicles or lipid bilayers rearranged from the unilamellar vesicles,[18,19] but the amount of functional lipids on the targeted surfaces cannot be precisely controlled,

* Correspondence author. E-mail: mvaldez@correo.fisica.uson.mx; phone: +662 2592108; fax: +662 2592109.
[†] Departamento de Investigación en Polímeros y Materiales, Universidad de Sonora.
[‡] Universidad Autónoma de San Luis Potosí, Universidad de Sonora.
[§] Departamento de Investigaciones Científicas y Tecnológicas.
[||] Departamento de Física, Universidad de Sonora.

10.1021/jp902709t CCC: $40.75
Published on Web 07/01/2009

because phospholipids with different headgroups are heterogeneously distributed on the two leaflets of vesicles. In comparison with the lipid bilayers,[20] the proportion of different components in Langmuir monolayers can be precisely controlled. In this investigation line, different researchers have recently used modern molecular dynamics methods[21,22] in order to analyze the kind of pores that AMPs produce in lipid bilayers. Also, some investigators have used spectroscopic methods to find evidence of pores in oriented lipid membranes interacting with AMPs,[23] and recently Mahalka and Kinnunen[24] have reviewed the recent developments of the AMPs interaction with lipid bilayers.

The interaction of several AMPs with phospholipids at the air−water interface has been investigated in order to understand the way they eliminate different microorganisms.[2,25−27] Therefore, many researchers have focused their attention to understanding the effect of peptides and proteins on the different phases of phospholipid monolayers. The coexistence of the liquid-condensed (LC) and liquid-expanded (LE) phases in Langmuir monolayers of phospholipids and phospholipids−protein mixtures has been studied for a long time.[28] It is known that nonhorizontal isotherms going through the LE-LC phase transition is probably caused by surface-active impurities in most cases, even though alternative explanations have been put forward.[28,29] It has also been shown that in protein/lipid monolayers, proteins preferentially arrange in the LE phase of the monolayer.[30] Therefore, if the concentration of impurities increases then the isotherm will become less and less horizontal at the transition.[31] This is because the impurity is more soluble in one phase than in the other, normally in the LE phase; as the system is compressed the concentration of the impurity does not remain constant and continuously changes in each phase.

In spite of the fact that several studies have been performed to try to understand the interaction between bactenecin and the cytoplasmatic membrane,[12] and vesicles have been used as model to investigate the interaction with some member of the family of bactenecins,[32] as far as we know no investigations related with the interactions of bactenecin with phospholipid monolayers have been done.

In this work, we are interested in understanding the adsorption of the peptide bactenecin onto 1,2-dipalmitoyl-*sn*-glycero-3-phosphocholine (DPPC) monolayers at the air−water interface. Different salt (NaCl) concentrations were used in the subphase in order to investigate the effect of salt concentration on the peptide adsorption. We performed isotherms and compression−expansion cycles; Brewster angle microscopy (BAM) images were obtained in situ to visualize the effect of bactenecin on DPPC domain structure. Atomic force microscopy (AFM) images were obtained for different Langmuir−Blodgett films obtained from DPPC/bactenecin mixtures to determine microstructure changes on DPPC LC-LE phase coexistence.

2. Experimental Section

Materials. Dodecapeptide bactenecin with sequence H−Arg−Leu−Cys−Arg−Ile−Val−Val−Ile−Arg−Val−Cys−Arg−OH (Disulfide bridge: 3−11), from bovine, was purchased from American Peptide Company (98.5% purity and 82.1% peptide content) and dissolved in trifluoroethanol (TFE) from SIGMA (USA); 1,2-Dipalmitoyl-*sn*-Glycero-3-Phosphocholine (DPPC) was obtained from Avanti Polar Lipids (Alabaster, AL., USA), and both were used without further purification. NaCl was purchased from SIGMA (USA) and baked in an oven at 300 °C for 2 h before use. Chloroform (HPLC grade) was obtained from SIGMA Aldrich (USA). Water was filtered with an Easy pure/Barnstead instrument with a resistivity of 18.3 MΩ·cm. DPPC was dissolved in chloroform at a final concentration of 1 mg/mL and the appropriate amounts of DPPC was spread on the Langmuir trough surface. Bactenecin was dissolved in TFE at final concentration of 1 mg/mL. As a subphase, we used different NaCl concentrations: 0.01, 0.05, 0.1, and 0.5 M. Temperature was kept at 20 °C using a water circulator bath (Cole-Palmer, 1268−24, USA).

Isotherms and Langmuir−Blodgett Monolayers. A Langmuir balance (Nima Technologies, Ltd., Coventry, England, Langmuir−Blodgett trough, Model type 611), whose surface tension precision is 0.1 mN/m, was employed to obtain DPPC isotherms modified with different NaCl solutions in the aqueous subphase and to obtain DPPC/bactenecin isotherms with the same subphase conditions applied to DPPC Langmuir isotherms. The surface pressure $\pi = \gamma_o - \gamma$, that is, the surface tension difference of the clean water surface and the covered surface, was measured using the Wilhelmy plate method. The surface pressure and molecular area data were fed into a computer and recorded, using a barrier speed of 20 cm^2/min. Each DPPC sample (50 μL) was spread on a clean water surface with a Hamilton microsyringe, and the peptide was injected into the subphase to achieve a final concentration of 10^{-4} mg/mL. All experiments were carried out inside a dust-free glass box. We also performed 1 mg/mL DPPC/bactenecin mixtures dissolved in chloroform and spread onto the through surface in a 60:40 wt/wt ratio, using the same conditions described above.

After the surface was cleaned, DPPC was spread on the subphase (500 mL) at a pressure lower than 0.1 mN/m. Isotherms were performed 15 min after DPPC was spread to allow chloroform evaporation and 4 h after 50 μL of the bactenecin solution was injected into the subphase to let the peptide molecules diffuse from the bulk to the DPPC Langmuir monolayer; the DPPC monolayer was deposited on subphases with different salt concentrations previous to the peptide injection. Isotherms were repeated three times with an average relative error of 2%.

Compression−expansion cycles for DPPC and DPPC/bactenecin monolayer's were performed 4 h after DPPC was spread on the surface and bactenecin was injected in subphases with 0.01 and 0.5 M NaCl solutions. The maximum pressure was kept at 20 mN/m to prevent the collapse of the lipid monolayer and to perform the experiments near the DPPC LE-LC coexistence.

Atomic Force Microscopy. DPPC and DPPC/bactenecin Langmuir−Blodgett films were obtained on freshly cleaved mica from different salt concentrations in the subphase. Monolayers were extracted at different surface pressures at a speed of 1 mm/min. Also DPPC/bactenecin films were transferred from DPPC/bactenecin mixtures deposited on the water surface as explained above.

A JEOL instrument (JSPM 4210, Japan) and an AFM (Digital, Mod. Nanoscope IIIa, USA) were used for imaging in the noncontact and tapping modes, respectively, using silicon nitride cantilevers NSC15 from MicroMash (USA) at room temperature.

Brewster Angle Microscopy. A Brewster angle microscope (BAM) using an objective of 10× (Mod. I-ELLI 2000; Nanofilm Technology GmbH) was used to obtain DPPC and DPPC/bactenecin images in situ. Images were recorded and computer analyzed using appropriate software from Nanofilm Technology GmbH. DPPC and DPPC/bactenecin images were obtained at different times, surface pressures, and salt concentrations in the subphase.

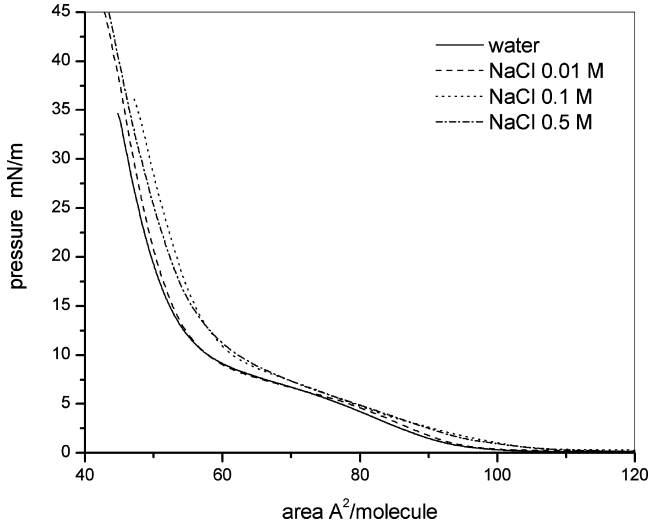

Figure 1. Isotherms of DPPC on different NaCl concentrations in the subphase at 20 °C.

3. Results and Discussion

Isotherms and Compression−Expansion Cycles. DPPC isotherms were performed using different NaCl concentrations between 0.01 and 0.5 M in the subphase. As can be observed in Figure 1, the presence of NaCl shifted the isotherms to higher surface pressures. This behavior was also observed by Aroti et al.[33,34] using different sodium salt solutions. They observed a systematic shift in the isotherms and large pressure changes for high areas when using NaI as subphase. In our case, we noticed relatively large changes at low surface pressures and high areas. Our pressure values measured at 85 Å/molecule were similar but a little lower in comparison to the ones found by Aroti et al., probably because they used a higher subphase temperature. Another interesting feature is that the pressure increase is not monotonic with salt concentration for all areas in the isotherms. At lower areas, pressure values are larger for 0.1 M than the ones for 0.5 M; and at higher areas, differences are negligible. The extrapolated area in the condensed phase changes from 55 Å/molecule for the subphases with pure water and 0.01 M salt concentration to around 58 A^2 for the subphases with 0.1 and 0.5 M salt concentrations. This small shift could be due to a stabilization of the LE phase due to ion insertion,[33] shifting the appearance of the LE phase to higher areas and pressures, which results also in a shift to larger areas of the LE-LC coexistence region. We notice also that a smaller plateu is observed with the salt concentration; this is contrary to the effect produced by a NaI solution as subphase found by Aroti et al.[33] This behavior will be better understood by comparing the compressibility of the monolayers with the different salt concentrations in the subphase.

Figure 2a shows DPPC isotherms with different salt concentrations in the subphase obtained 4 h after bactenecin was injected into the subphase. We observe a pressure increment for a fixed molecular area caused by the peptide adsorption with and without salt in the subphase. It is interesting to observe the absence of the characteristic plateu corresponding to the DPPC LE-LC coexistence region. However, higher pressures are reached for the lowest salt concentration used (0.01 M) in comparison with the pressure obtained in the isotherm for the 0.5 M salt concentration in the subphase. Unexpectedly, this last isotherm shows more similarities with the DPPC isotherm obtained when bactenecin is adsorbed into the interface from a pure water subphase. This effect could be explained by assuming

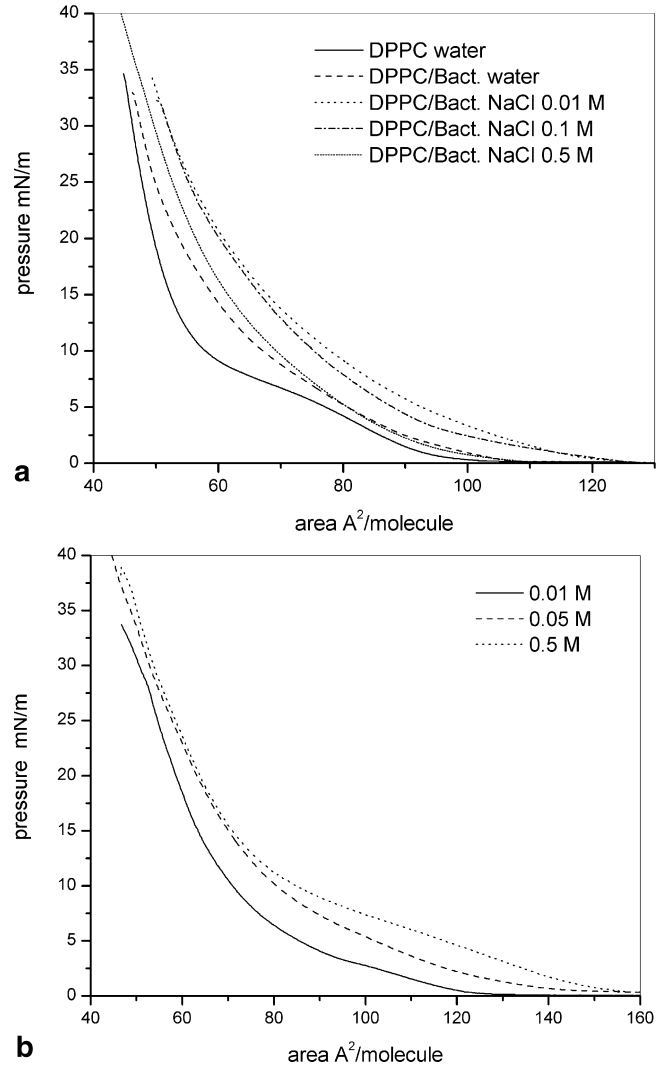

Figure 2. Isotherms of DPPC/bactencin obtained with two different methods: (a) Isotherms of DPPC/bactenecin monolayers obtained 4 h after bactenecin was injected into the subphase. Different salt concentrations are indicated. Solid line represents the DPPC isotherm on a pure water subphase as reference. (b) DPPC/bactenecin isotherms over different salt concentration subphases, obtained by spreading a DPPC/bactenecin mixture (60:40 wt/wt).

that higher salt concentrations in the subphase decreases the Debye constant and therefore, phospholipids at the interface remains closer to Cl^{1-} ions, building an electrostatic barrier formed by Na^{1+} contra-ions, thus lowering the cationic peptide adsorption at the interface. On the contrary, low and moderate salt concentrations increases the Debye constant, between 5 and 10 times; therefore, the negative charge at the interface allows easier adsorption of the cationic peptide.[35,36]

The limiting area A_0 (determined by extrapolation at the intersection of the abscissa axis with the tangent of the isotherm at 2 mN/m), is increased from 95 (pure water subphase) to 103 $Å^2$/molecule for the DPPC/bactenecin isotherm when water/bactenecin is the subphase, whereas the values of A_0 for 0.01 and 0.1 M salt concentration in the subphase are increased more than 15 $Å^2$/molecule as a consequence of the DPPC/bactenecin interaction. The effect of the peptide intercalation in the DPPC monolayer can also be observed at lower areas. For the extrapolated area in the LC phase the values increased up to 67 $Å^2$/molecule due to the combined effect of the salt and the peptide interaction, which means an approximate increment of 10 $Å^2$/molecule with respect to the pure DPPC monolayer. The

pressure increment due to the peptide penetration, measured at the middle of the DPPC LC-LE coexistence region, can be observed in Figure 2a. We obtain 16.7 mN/m for the 0.01 M isotherm in comparison with 7.7 mN/m obtained at 65 Å^2 for the DPPC isotherm with pure water as subphase. As can be observed, the net effect of the DPPC/bactenecin interaction is the absence of the known LE-LC coexistence region plateau, also observed in DPPC monolayers penetrated by bovine serum albumin molecules.[37] However, since now the monolayer is made of more than one component, the LE-LC coexistence still exists, as we show below by BAM and AFM images, even though no plateau is observed.

According to the results of Aroti et al.,[33] there is a preferential adsorption of the Cl^{1-} anions compared with the Na^{1+} cations in the DPPC headgroup region, resulting in a negative charged monolayer that causes the pressure increment in the LE phase. The negative monolayer increases the attraction of cationic peptides, producing a new pressure increase. On the other hand, for higher salt concentrations, we could obtain a screening effect at the monolayer, lowering the attraction between the monolayer and the cationic peptide bactenecin as can be observed in Figure 2a for the isotherm obtained with 0.5 M salt concentration in the subphase.

From the isotherms shown in Figure 2a we notice that the adsorption of bactenecin does not contribute to a new phase, as is the case for albumin and other proteins penetrating lipid monolayers near 20 mN/m by several authors,[37−41] probably due to size difference or to differences of the adsorption properties. That is, the peptide could easily fit between the phospholipid headgroup without greatly increasing the area occupied by the headgroup.

Isotherms of DPPC/bactenecin mixtures in chloroform were also performed by spreading the solutions over different salt concentration subphases. Figure 2b shows the effect of the salt concentration on the isotherm shifts at higher areas, similar to the effect observed in Figure 1 for pure DPPC monolayers. Notice also that at higher pressures, the shift of extrapolated areas in the condensed phase is similar to the effect observed in Figure 2a, where peptide molecules were adsorbed in the DPPC monolayer from the subphase. Another difference found at higher pressures is that collapse begins at relative low surface pressures not observed in Figure 2a but observed for protein monolayers by other authors.[40] This behavior is probably caused by the differences in the peptide destabilization of the DPPC monolayer.

Around the DPPC LE-LC coexistence region (65 Å^2/molecule), the pressure increase is similar to the increase observed in Figure 2a. However, this coexistence is not completely eliminated, even with the highest salt concentration used in the subphase. This behavior is quite different to the one observed in Figure 2a, where the LC-LE coexistence region plateau is practically eliminated and is similar to the behavior observed by Diociaiuti et al.[42] by mixing the polypeptide gramicidin (15 aminoacids) with DPPC at the air/water interface. According to their aggregation model, gramicidin builds aggregates like small islands surrounded by DPPC molecules. These aggregates grow with the peptide concentration, but the LE-LC equilibrium is not completely destroyed. Therefore, the change of the LE-LC coexistence region in Figure 2a could be caused by a random intercalation/penetration of bactenecin molecules and further formation of a mixture of the bactenecin with the DPPC monolayer.[43]

The results obtained for the DPPC monolayers and the DPPC/bactenecin monolayers over subphases with different salt concentrations were analyzed with the compressibility of monolayers $C_s = -(1/A)((\partial A)/(\partial \pi))_T$, where A and π are the molecular area and the surface pressure, respectively.

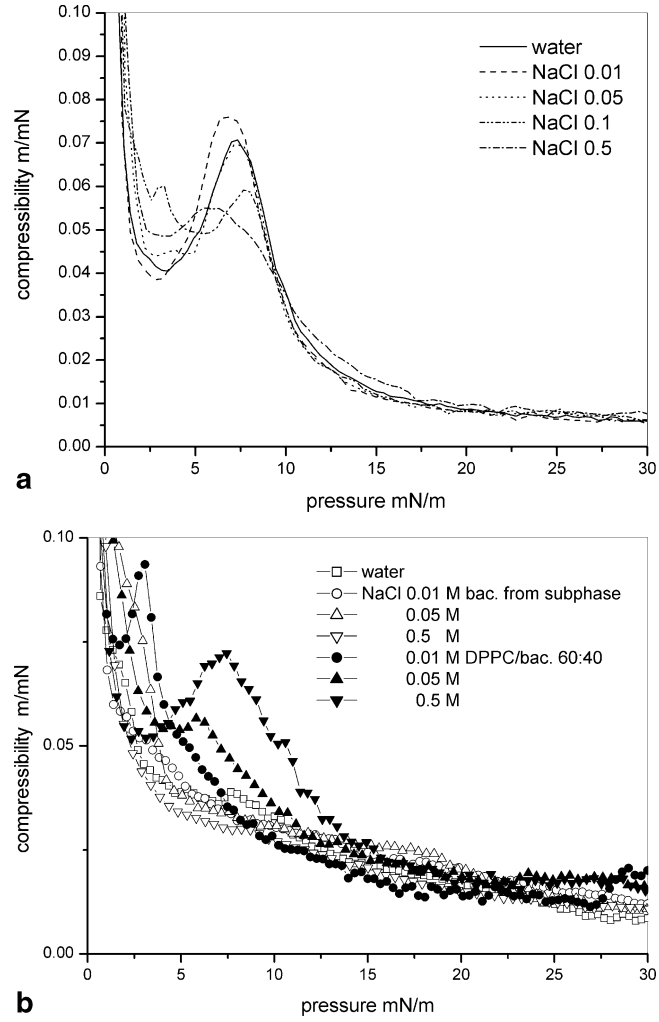

Figure 3. Compressibility curves of DPPC/bactencin monolayers obtained with different salt concentration in the subphase. (a) Compressibility curves for DPPC monolayers obtained from isotherms given in Figure 1. (b) Compressibility curves of DPPC/bactenecin monolayers over different subphases obtained from isotherms given in Figure 2, panels a and b.

The compressibility of DPPC monolayers were measured long time ago.[44] These authors found a value of 1.2×10^{-2} m/mN at 5 mN/m and 0.9 m/mN in the LC phase at $\pi \approx 15$ mN/m. Recently, Duncan and Larson[45] reviewed many of the results of different compressibility values found by different authors using different experimental conditions and concluded that compressibility values ranged between 0.004 and 0.01 m/mN in the LC phase and between 0.02 and 0.1 m/mN in the LE phase. Our C_s values for DPPC monolayers can be observed in Figure 3a, where C_s varies from 0.04 to 0.1 m/mN in the LE phase and from 0.006 to 0.02 m/mN approximately in the LC phase. Notice the effect of salt in the LE-LC coexistence region, where C_s reaches a maximum value and this maximum decreases with salt concentration. This means that more rigid DPPC monolayers are obtained for higher salt concentrations in the subphase at the coexistence region. Differences are smaller in the LC phase, showing almost the same C_s value without significant influence of salt concentration, corroborating the results of Aroti et al.;[33] that is, anions do not penetrate DPPC monolayers in the condensed phase.

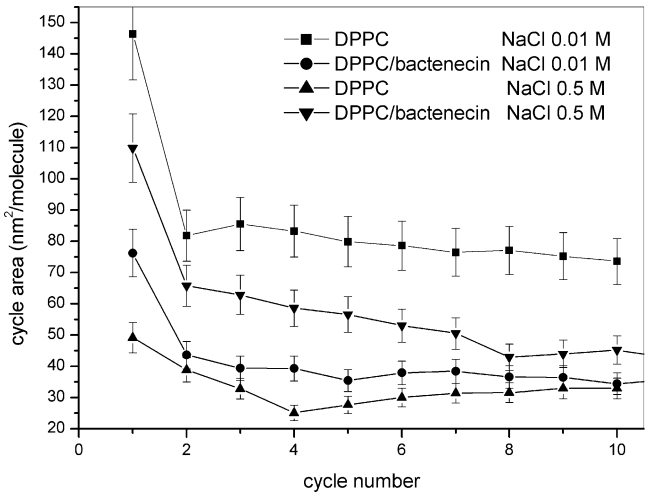

Figure 4. Area of the compression−expansion cycles of DPPC and DPPC/bactenecin monolayers for different cycles and for two different salt concentrations in the subphase. Temperature was kept at 20 °C. DPPC/bactenecin cycles were performed 4 h after the peptide was injected.

Figure 3b shows the C_s values for the DPPC/bactenecin monolayer, obtained from curves in Figure 2a and 2b. For the case of monolayers obtained by the bactenecin adsorption from the subphase and for lower pressures in the G (gaseous) and LE phases, C_s values are similar to the ones observed in Figure 3a. However, the elimination of the peak corresponding to the LE-LC coexistence appears clearly for all salt concentrations. We observe a small vestige of the peak corresponding to the DPPC/bactenecin monolayer with a pure water subphase. This could mean that both peptide penetration and ionic strength contribute to the absence of the LE-LC coexistence plateau. As the pressure increases above 15 mN/m, the C_s values slowly decrease but are almost twice as big (0.01 m/mN) in comparison with the values given in Figure 3a. Notice also that compressibility at higher pressures is practically independent of the salt concentration, also observed for DPPC alone.

The behavior of the compressibility of DPPC/bactenecin monolayers determined from curves in Figure 2b is shown also in Figure 3b. Compressibility values showed a small relative maximum corresponding to the LE-LC equilibrium of DPPC monolayers when no salt is added. This behavior of the compressibility monolayer is in accordance to our discussion about the peptide interaction/penetration of the monolayer expressed above. It is interesting noting that at higher pressures, the C_s values for all salt concentrations used are similar to the ones obtained for the DPPC/bactenecin monolayers when bactenecin molecules are adsorbed from the subphase. This could mean that when DPPC enters the LC one-phase region, bactenecin molecules interact with DPPC molecules independent of the way they arrived to the interface.

Figure 4 shows the time evolution of the area of different compression−expansion cycles for DPPC and DPPC/bactenecin monolayers over 0.01 and 0.5 M salt concentration solutions in the subphase (peptide molecules were adsorbed from the subphase). The behavior of cycles with DPPC alone has been reported[37] without salt in the subphase. The result is similar to the one shown in Figure 4 for two salt concentrations. However, the area change after 10 cycles observed in Figure 4 for DPPC with the 0.01 M salt concentration subphase, was around 50% in comparison with the 30% observed for a pure water subphase.[37] This last value is similar to the 32% area change for DPPC with 0.5 M salt in the subphase, in accordance also with the similarities of the corresponding isotherms in Figure 1. The irreversibility of the squeeze out of phospholipids during compression at high pressures was also observed by Takamoto et al.[46] using DPPG and DPPG-POPG mixtures, pointing out that lipids in the subphase formed three-dimensional structures that did not return to the interface at lower pressures.

Investigations on the influence of proteins in the reversibility of the squeeze out of phospholipids to the subphase have been reported.[35,46−49] The interaction of DPPC with human serum albumin was investigated by Li et al.[47] They performed cycles of DPPC/serum albumin and found that the protein was squeezed out completely at pressures higher than 30 mN/m, but at lower pressures protein molecules returned again and mixed with the lipid at the interface. The influence of some pulmonary proteins on the return of phospholipids to the interface was investigated by Takamoto et al.,[46] who found similar results.

We found that for DPPC and DPPC/bactenecin monolayers, the largest expulsion of molecules from the interface took place from the first to the second cycle, where more than 40% of the area was lost, except for the 0.5 M salt concentration subphase, where only 22% of the original area was lost. Therefore, the combined effect of salt concentration and peptide molecules in the interface produce smaller cycled areas, indicating a weak DPPC/bactenecin interaction as has been pointed out by Merzlyakov et al.,[48] who suggested that a larger hysteresis area indicates strong protein−protein or/and DPPC−protein interactions. According to the results observed by Alig et al.[35] with DPPC/BSA monolayers, it is probable that both cationic peptides and salt ions saturate the interface, inhibiting the return of DPPC to the interface and producing compression−expansion cycles with smaller areas.[49]

Brewster Angle Microscopy. The morphology of pure DPPC and DPPC/bactenecin was observed under different subphase conditions at the air/water interface. BAM images were taken during the monolayer compression at 20 °C on water and some NaCl concentrations. At low surface pressures, c.a. 4−5 mN/m, keeping the pressure constant after 1 h, all images looked similar, showing small bright speckles on a dark background. When using pure water as the subphase, at 10 mN/m after 1 h, DPPC showed small and dense heterogeneous structures around the LE-LC coexistence region as observed in Figure 5a. Note that at longer times (4 h) and at the same pressure, DPPC forms a variety of bigger structures that form diverse shapes already found by different researches,[31,33,50,51] known as triskelions, see Figure 5b.

At low pressures the effect of the peptide absorption on the DPPC monolayer was not appreciated after 1 h and was similar as in the case of DPPC on pure water. However, after 1 h at 10 mN/m, as observed in Figure 5c, dense star-like structures appear in comparison with the images obtained for DPPC alone in Figure 5a. Note also that the domains are smaller than the ones obtained for pure DPPC at the same conditions. This shrinking of the DPPC LC phase domains caused by peptides at the air−water interface was also demonstrated by Bonardia et al.[50] Differences seem to be more pronounced at longer times, as observed in Figure 5d, as rounding of the domains sets in; since rounding of LC domains of pure DPPC monolayers takes much longer, we think that the rounding observed is a consequence of the peptide−DPPC interactions/penetration,[33] which could lower the quasi-long-range order of the LC phase allowing a faster molecular reorganization of the LC domains. It is interesting to notice that at longer times DPPC/bactenecin domains are bigger than the ones of pure DPPC. Therefore, it is probable that the condensation process of DPPC/peptide

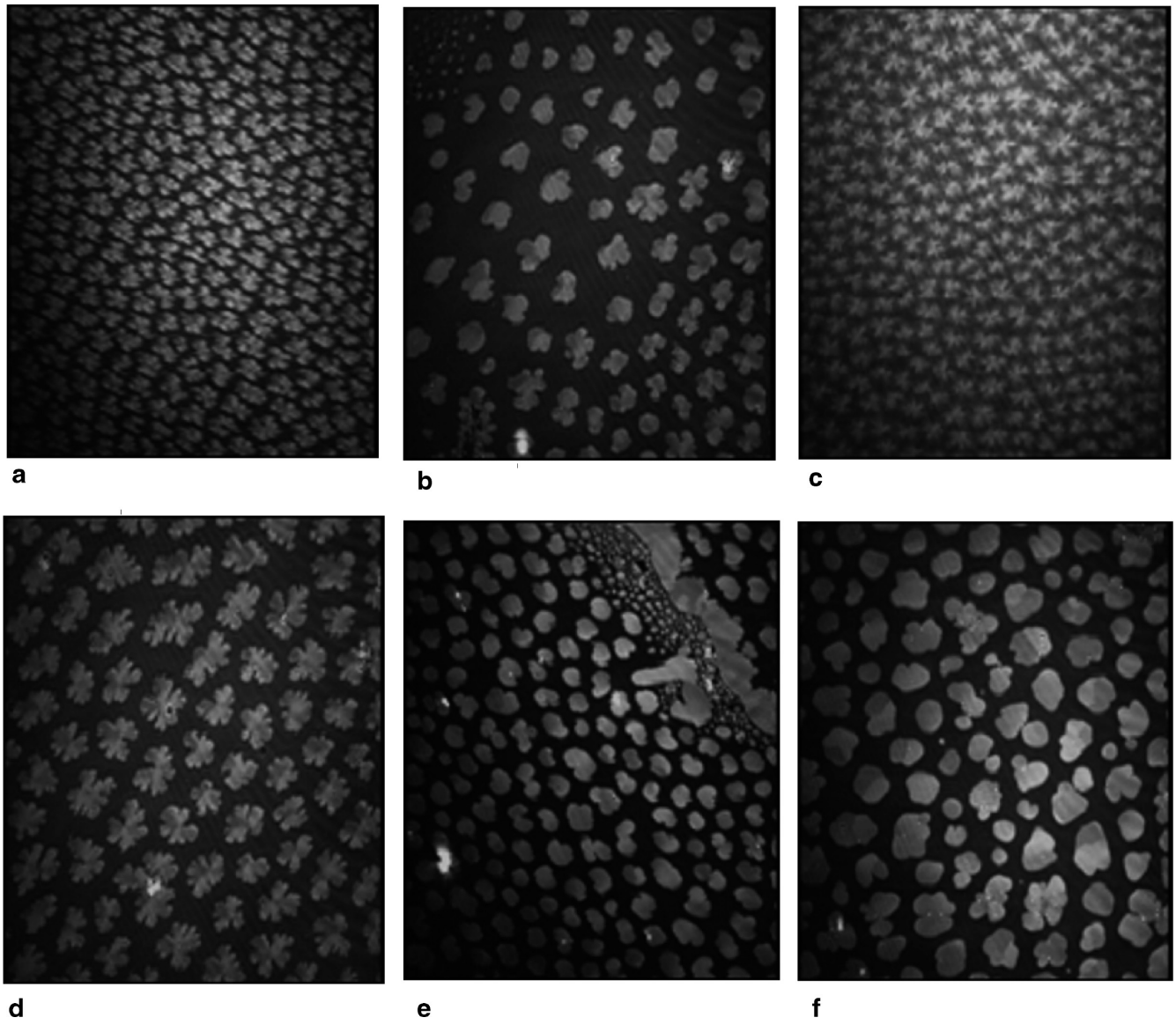

Figure 5. BAM images of DPPC and DPPC/bactenecin monolayers, observed at different times over different subphases at 10 mN/m. (a) DPPC 1 h after it was spread on a pure water subphase. (b) DPPC 4 h after it was spread on a pure water subphase. (c) DPPC/bactenecin 1 h after bactenecin was injected into a pure water subhase. (d) DPPC/bactenecin, 4 h after the peptide was injected into pure water subphase. (e) DPPC 4 h after it was spread on a 0.5 NaCl concentration subphase. (f) DPPC/bactenecin, 4 h after bactenecin as injected into a 0.5 M NaCl concentration subphase. Image sizes are 462 × 564 μm.

domains is slower than for pure DPPC domains, since the peptide molecules have to diffuse from the bulk and this transport process could be quite slow.[52−54]

For low salt concentration and low surface pressure, the structures or domains seemed to be similar to the DPPC domains with pure water as subphase, but as the salt concentration was increased, the size of the domains observed at 4−5 mN/m were bigger after 1 h in comparison with the morphologies without salt or with low salt concentration (not shown). Therefore, the salt could contribute to build DPPC nucleation sites. Around 10 mN/m, the DPPC image for the 0.01 M salt concentration (not shown) was similar to the one shown in Figures 5a and 5b for pure water as subphase. The diversity of size and shapes of domains decreased for the higher salt concentration subphase, as can be observed in Figure 5e for NaCl 0.5 M in the subphase. The domain structures are disk-like instead of the more elongated structures observed on pure water or in low salt concentrations, probably as a consequence of the higher hydrophobic interactions in comparison with the electrostatic forces.[33]

The combined effect of salt and adsorbed peptides at the DPPC monolayer is observed after 4 h in Figure 5f. We observe structures with rounded edges; however, the average size of the domains was bigger in comparison with those observed in Figure 5e, probably due to the nucleation effect of the salt. Also note that domains in all images of Figure 5 have internal structure due to molecular tilt. This indicates that the domains correspond to a LC phase of DPPC, which means that even though the LC-LE coexistence plateau disappears in the isotherms due to the presence of salt or bactenecin, the LE and LC phospholipid phases are still present. This is the case in our experiments where bactenecin acts as an impurity, which is more soluble in the LE phase. However it does not mean that the LC-LE coexistence disappeared, since our BAM results show its presence, but the isotherm is no longer flat at the LC-LE coexistence region. Similar isotherm behavior has been reported for the LC-LE transition for some phospholipids and proteins or peptide mixtures at the air−water interface,[54−58] and it has been mentioned that even when no coexistence plateau was observed, they have obtained this LC/LE transition. Results

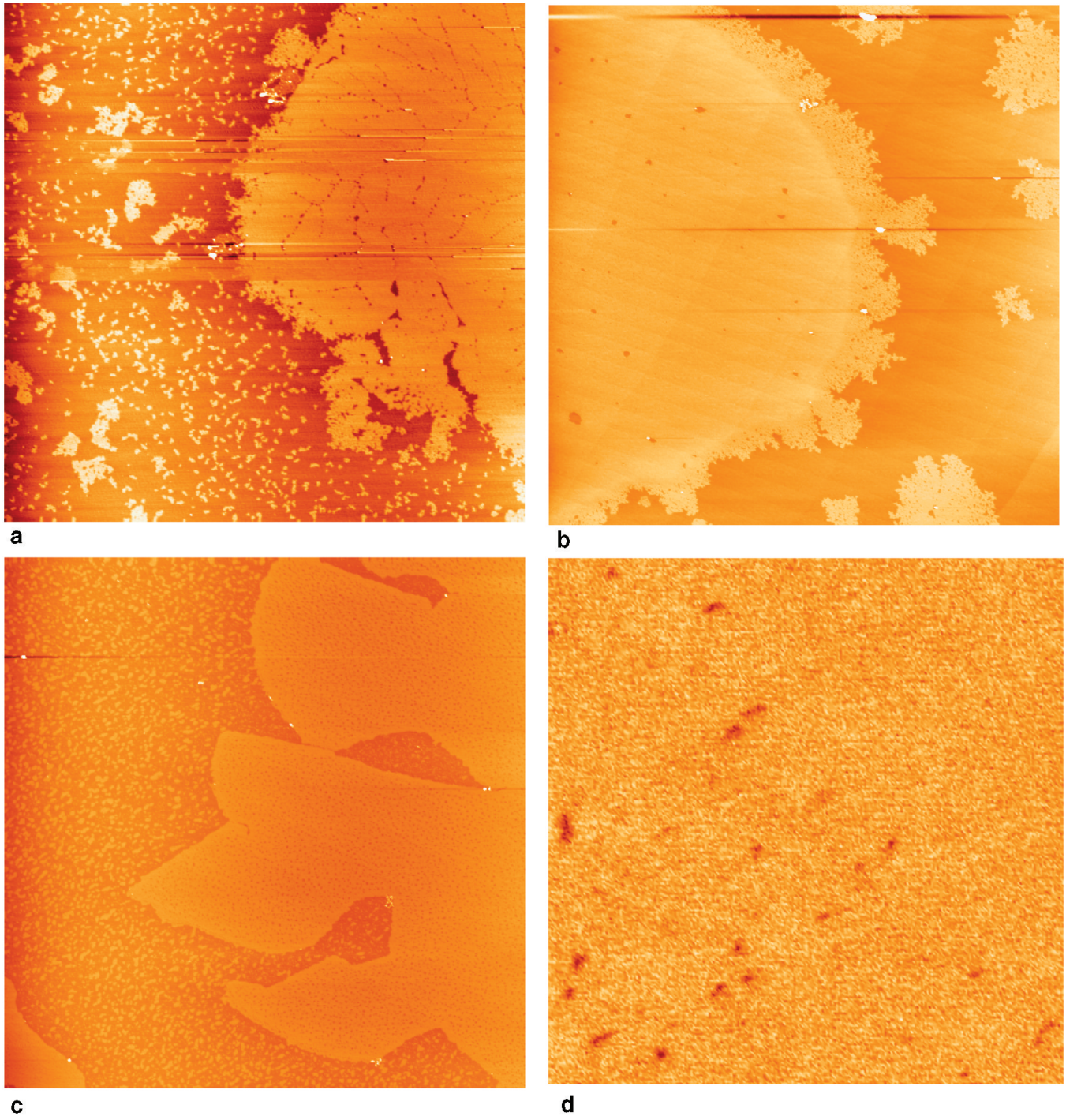

Figure 6. AFM images of DPPC and DPPC/bactenecin LB films transferred on mica at 10 mN/m from different subphases. (a) DPPC on 0.01 M salt concentration ($7 \times 7\ \mu m^2$), (b) DPPC on 0.5 M salt concentration ($8 \times 8\ \mu m^2$), (c) DPPC/bactenecin on 0.01 M salt concentration ($10 \times 10\ \mu m^2$), and (d) DPPC/bactenecin on 0.5 M salt concentration ($2 \times 2\ \mu m^2$).

obtained by Nakamura et al.,[31] using both fluorescence microscopy and BAM, mixing DPPC and different concentrations of fluorinated amphiphiles at the air−water interface showed that the order/disorder coexistence state is reached at low pressure and beyond 35 mN/m near the collapse of the monolayer without a coexistence plateau in the isotherms.

AFM Images. Figure 6 shows results of DPPC and DPPC/bactenecin Langmuir−Blodgett films obtained at 10 mN/m from 0.01 and 0.5 M NaCl solutions in the subphase. The effect of 0.01 M Nacl is shown in Figure 6a, where LC (bright homogeneous domains) and LE regions (dark continuous areas) are observed. Note the formations of aligned holes in the bigger LC domain. Also note that the edge of the big LC domain is quite disordered and that there a large number of small LC domains around it; the small domains look like debris that separated from the big domain. The effect of the salt concentration in the subphase is shown in Figure 6b where 0.5 M salt concentration was used in the Langmuir balance. We noted that the LC and LE domains were more homogeneous and that LC domains have much less holes on their surface, in good agreement with isotherm results, where the effect on isotherms was bigger at lower concentration of salt. However, note that a floppy edge is still present on the big domain, but the smaller domains are much bigger that the debris seen in Figure 6a.

The effect of the peptide adsorption in the DPPC monolayer is shown in Figure 6c for the 0.01 M salt concentration in the subphase. It seems that the peptide adsorption in the LE regions with small sparkles causes that now the average height size of this region ranges between 0.5 and 1.2 nm, measured from the mica surface. Remarkably, the big LC region contains a high density of holes produced by the bactenecin; it is clear that bactenecin penetrates the LC phase to form holes, as providing direct evidence of its antibiotic capacity. Holes produced due to the AMPs interaction with biological membranes and phospholipid bilayers have been widely investigated by different researchers.[21−24] The height profile of the LC region varies from 0.6 to 2.5 nm heights, similar to the value found by other authors.[37,59] The adsorption of bactenecin on the monolayer, and especially on the LC phase, is affected by increasing the salt concentration in the subphase. Figure 6d shows that the increase of salt decreases the number of holes produced by bactenecin on the LC phase, as the surface of the LC domains look smooth. We think that as the salt concentration increases, a cationic barrier is formed near the interface impeding the cationic peptide to reach the DPPC mononalayer. In addition, fractal-like shapes of the edges of the LC domains were observed for DPPC/bactenecin structures with pure and low salt concentration in the subphase, similar to the observations performed by BAM, probably caused by higher electrostatic interactions.

4. Conclusions

In this paper we presented the effect of the interaction of the cationic peptide bactenecin with a DPPC Langmuir monolayer in the presence of salt; we obtained isotherms of DPPC and DPPC/bactenecin monolayers at the air−water interface over different NaCl concentrations in the subphase. The salt concentration perturbed strongly the LC-LE coexistence regions of DPPC monolayers, obtaining shifted isotherms and more rigid films around the LC-LE equilibrium. The adsorption of bactenecin from the subphase into DPPC monolayers was influenced by the NaCl concentration. Remarkably, a bigger effect of bactenecin is obtained on the isotherms at low salt concentration rather than at higher one; as the salt concentration increases, it forms an electrostatic barrier that impedes bactenecin reaching the monolayer. The compressibility of DPPC/bactenecin films showed that NaCl in the subphase produced a more extended LE phase and the disappearing of the LC-LE coexistence plateau, contrary to the effect of DPPC/bactenecin monolayers obtained by depositing DPPC/bactenecin mixtures on the interface, where the LC-LE coexistence plateau did not disappeared. This can be understood because in the first type of experiments bactenecin penetrates and became part of the monolayer, which is now formed by more than one component, and one should not expect the presence of a flat coexistence plateau. In the second set of experiments, bactenecin could easily fit between the lipid chains not forming part of the monolayer, therefore affecting marginally the LC-LE transition. Indeed, the presence of the LC-LE coexistence was corroborated by BAM and AFM observation, where in all experiments LC and LE domains where observed. Compression−expansion cycles of DPPC/bactenecin monolayers showed that the combined effect of salt and peptide produced small area hysteresis, probably because higher salt concentration built an electrostatic barrier that inhibited the return of peptide molecules to the interface. Even though the DPPC−bactenecin interaction showed to be relative weak, the BAM observations showed that some kind of interaction was observed, specifically at the LC-LE coexistence region. AFM observations showed the LC domains were greatly affected by the bactenecin adsorption, particularly for low salt concentrations in the subphase, where a great number of holes are observed on the LC domains. Neither BAM nor AFM could detect the effect of bactenecin absorption on the LE phase, but the shift on the isotherms in the pure LE phase clearly indicated that bactenecin was absorbed, however. By contrast, at high salt concentrations an electrostatic barrier seem to prevent a large number of bactenecin molecules reaching the interface, since the number of holes on the LC domains is greatly decreased. In summary, we have shown the effect of salt concentration and of the antibiotic bactenecin on a model DPPC membrane at the air/water interface. We show that the Langmuir technique along with BAM and AFM observations are complementary for evaluating the effect of peptide antibiotics.

Acknowledgment. The Consejo Nacional de Ciencia y Tecnología (CONACyT) is gratefully acknowledged for grants SEP-2004-CO1-46749 and 60833. A.B.L.O. and A.L.F.V. acknowledge a Ph.D. and a Postdoctoral scholarship from CONACYT, respectively.

References and Notes

(1) Boman, H. G. *Annu. Rev. Inmmunol.* **1995**, *13*, 61–65.
(2) Hancock, R. E.; Scott, M. G. *Proc. Natl. Acad. Sci. U.S.A.* **2000**, *97*, 8856–8861.
(3) Zasloff, M. *Nature* **2002**, *415*, 389–395.
(4) Rosenfeld, Y.; Shai, Y. *Biochim. Biophys. Acta* **2006**, *1758*, 1513–1522.
(5) Agerberth, B.; Gunne, H.; Odelberg, J.; Kogner, P.; Boman, H. G.; Gudmundsson, G. H. *Procl. Natl. Acad. Sci. U.S.A.* **1995**, *92*, 195–199.
(6) Cole, A. M.; Kim, Y. H.; Tahk, S.; Hong, T.; Weis, P.; Warning, A. J.; Ganz, T. *FEBS Lett.* **2001**, *504*, 5–10.
(7) Hanckock, R. W.; Chapple, D. S. *Antimicrob. Agents Chemother.* **1999**, 1317–1323.
(8) Moore, K. S.; Bevins, C. L.; Brasseur, M. M.; Tomassin, N.; Turner, K.; Eck, H.; Zasloff, M. *J. Biol. Chem.* **1991**, *266* (29), 19851–19857.
(9) Sung, W. S.; Park, Y.; Choi, C.; Hahm, K.; Lee, D. G. *Biochem. Biophys. Res. Commun.* **2007**, *363*, 806–810.
(10) Berisha, H.; Foda, H.; Sakakibara, H.; Trotz, M.; Pakbaz, H.; Said, S. I. *Am J. Physiol. Lung Cell Mol. Physiol.* **1990**, *259*, 151–155.
(11) Wu, M.; Hancock, R. E. W. *Antimicrob. Agents Chemother.* **1999**, *43*, 1274–1276.
(12) Wu, M.; Hancock, R. E. W. *J. Biol. Chem.* **1999**, *274*, 29–35.
(13) Friedrich, C. L.; Moyles, D.; Beveridge, T. J.; Hancock, R. E. W. *Antimicrob. Agents Chemother.* **2000**, *44* (8), 2086–2092.
(14) Romeo, D.; Skerlavaj, B.; Bolognesi, M.; Gennaro, R. *J. Biol. Chem.* **1988**, *263*, 9573–9575.
(15) Vylkova, S.; Sun, J. N.; Edgerton, M. *Purinergic Signall.* **2007**, *3*, 91–97.
(16) Brogden, K. A. *Nature* **2005**, *3*, 238–250.
(17) Zhang, L.; Rozek, A.; Hancock, R. E. W. *J. Biol. Chem.* **2001**, *276*, 35714–35722.
(18) Yang, T.; Baryshnikova, O. K.; Mao, H.; Holden, M. A.; Cremer, P. S. *J. Am. Chem. Soc.* **2003**, *125*, 4779.
(19) Bondurant, B.; Last, J. A.; Waggoner, T. A.; Slade, A.; Sasaki, D. Y. *Langmuir* **2003**, *19*, 1829.
(20) Johnson, S. J.; Bayerl, T. M.; McDermott, D. C.; Adam, G. W.; Rennie, A. R.; Thomas, R. K.; Sackmann, E. *Biophys. J.* **1991**, *59*, 289.
(21) Klingelhoefer, J. W.; Carpenter, T.; Sansom, M. S. P. *Biophys. J.* **2009**, *96*, 3519–3528.
(22) Huang, H. W. *Biophys. J.* **2009**, *96*, 3263–3272.
(23) Kim, C.; Spano, J.; Park, E.; Wi, S. *Biochim. Biophys. Acta* **2009**, doi:10.1016/j.bbamem.2009.04.017.
(24) Mahalka, A. K.; Kinnunen, P. K. J. *Biochim. Biophys. Acta* **2009**, doi:10.1016/j.bbamem.2009.04.012.
(25) Maget-Dana, R. *Biochim. Biophys. Acta* **1999**, *1462*, 109–140.
(26) Volinsky, R.; Kolusheva, S.; Berman, A.; Jelinek, R. Biochim. *Biophys. Acta* **2006**, *1758*, 1393–1407.
(27) Wu, M.; Maier, E.; Benz, R.; Hancock, R. E. W. *Biochemistry* **1999**, *38*, 7235–7242.
(28) Fischer, A.; Losche, M.; Möhwald, H.; Sackmann, E. *J. Phys., Lett.* **1984**, *45*, 785–791.
(29) Miller, A.; Helm, C. A.; Möhwald, H. *J. Phys. (Paris)* **1987**, *48*, 693–701.

(30) Möhwald, H. Phospholipid Monolayers in: *Handbook of Biological Physics*, Lipowsky, R., Sackman, E. Eds.; Elsevier Science B. V.: 1995; Vol 1, Ch 4.
(31) Nakamura, S.; Nakahara, H.; Krafft, M. P.; Shibata, O. *Langmuir* **2007**, *23*, 12634–12644.
(32) Nidome, T.; Tsuiki, M.; Tokunaga, Y.; Hatakeyama, T.; Aoyagi, H. *Bull. Chem. Soc. Jpn.* **2000**, *73*, 1397–1402.
(33) Aroti, A.; Leontidis, E.; Maltseva, E.; Brezesinski, G. *J. Phys. Chem. B.* **2004**, *108*, 15238–15245.
(34) Aroti, A.; Leontidis, E.; Dubois, M.; Zemb, T. *Biophys. J.* **2007**, *93*, 1580–1590.
(35) Alig, T. F.; Warriner, H. E.; Lee, L.; Zasadzinski, J. A. *Biophys. J.* **2004**, *86*, 987–904.
(36) Dill, K. A.; Bromberg, S. *Molecular Driving Forces: Statistical Thermodynamics in Chemistry and Biology*; Garland Science, Taylor & Francis Group: New York and London, 2003.
(37) Valencia-Rivera, D. E.; Básaca-Loya, A.; Burboa, M. G.; Gutiérrez-Millán, L. E.; Cadena-Nava, R. D.; Ruiz-García, J.; Valdez, M. A. *J. Colloid Interface Sci.* **2007**, *316*, 238–249.
(38) Wang, X.; He, Q.; Zheng, S.; Brezesinski, G.; Möwald, H.; Li, J. *J. Phys. Chem. B* **2004**, *108*, 14171.
(39) Zasadzinski, J. A.; Alig, T. F.; Alonso, C.; de la Serna, J. B.; Perez-Gil, J.; Taeusch, H. W. *Biophys. J.* **2005**, *89*, 1621–1629.
(40) Sánchez-González, J.; Ruiz-García, J.; Gálvez-Ruiz, M. J. *J. Colloid Interface Sci.* **2003**, *267*, 286.
(41) Xicohtencatl-Cortes, J.; Mas-Oliva, J.; Castillo, R. *J. Phys. Chem. B* **2004**, *108*, 7307–7315.
(42) Diociaiuti, M.; Bordi, F.; Motta, A.; Carosi, A.; Molinari, A.; Arancia, G.; Coluzza, C. *Biophys. J.* **2002**, *82*, 3198–3206.
(43) Xicohtencatl-Cortes, J.; Castillo, R. M.-O. *J. Biochem. Biophys. Research Communications* **2004**, *324*, 467–470.
(44) Alsina, M. A.; Mestres, C.; Rabanal, F.; Busquets, M. A.; Reig, F. *Langmuir* **1993**, *9*, 1129–1133.
(45) Duncan, S. L.; Larson, R. G. *Biophys. J.* **2008**, *94*, 2965–2986.
(46) Takamoto, D. Y.; Lipp, M. M.; von Nahmen, A.; Lee, K. Y. C.; Waring, A. J.; Zasadzinski, J. A. *Biophys. J.* **2001**, *81*, 153–169.
(47) Li, J. B.; Zhao, J.; Wu, J.; Miller, R. *Narhung* **1998**, *42*, 232–233.
(48) Merzlyakov, M.; Li, E.; Hristova, K. *Langmuir* **2006**, *22*, 1247.
(49) Warriner, H. E.; Ding, J.; Waring, A. J.; Zasadzinski, J. A. *Biophys. J.* **2002**, *82*, 835.
(50) Bonardia, C.; Mendonca, C. R.; Campana, P. T.; Lottersberger, J.; Tonarelli, G.; Oliveira, Jr., O. N.; Beltramini, L. M. *Colloids Surf., B* **2005**, *41*, 15–20.
(51) Lucero, A.; Rodríguez Niño, M. R.; Gunning, A. P.; Morris, V. J.; Wilde, P. J.; Rodríguez Patino, J. M. *J. Phys. Chem. B* **2008**, *112*, 7651–7661.
(52) Hernández-López, J. L.; Alvizo-Páez, E. R.; Moya, S. E.; Ruiz-Garcia, J. *J. Phys. Chem. B* **2006**, *110*, 23179–23191.
(53) Hernández-López, L.; Alvizo-Páez, E. R.; Moya, S. E.; Ruiz-Garcia, J. *Carbon* **2007**, *45*, 2448–2450.
(54) Moraes, M. L.; Bonardi, C.; Mendonca, C. R.; Campana, P. T.; Lottersberger, J.; Tonarelli, G.; Oliveira, Jr., O. N.; Beltramini, L. M. *Colloids Surf., B* **2005**, *41*, 15–20.
(55) Ma, J.; Koppenol, S.; Yu, H.; Zografi, G. *Biophys. J.* **1998**, *74*, 1899–1907.
(56) Weron′ski, K.; Busquets, M. A.; Girona, V.; Prat, J. *Colloids Surf., B* **2007**, *57*, 8–16.
(57) Nakahara, H.; Nakamura, S.; Lee, S.; Sugihara, G.; Shibata, O. *Colloids Surf., A* **2005**, *270*−*271*, 52–60.
(58) Plasencia, I.; Keough, K. M. W.; Perez-Gil, J. *Biochim. Biophys. Acta* **2005**, *1713*, 118–128.
(59) Cruz, A.; Vázquez, L.; Vélez, M.; Pérez-Gil, J. *Biophys. J.* **2004**, *86*, 308.

JP902709T